



Pliocene expansion of C₄ vegetation in the core monsoon zone on the Indian Peninsula

Ann G. Dunlea¹, Liviu Giosan², Yongsong Huang³

5 ¹Marine Chemistry & Geochemistry, Woods Hole Oceanographic Institution, Woods Hole, MA, 02543, USA

²Geology & Geophysics, Woods Hole Oceanographic Institution, Woods Hole, MA, 02543, USA

³Department of Earth, Environmental, and Planetary Sciences, Brown University, Providence, RI, 02912, USA

Correspondence to: Ann G. Dunlea (adunlea@whoi.edu)

Abstract. The expansion of C₄ vegetation during the Neogene was one of the largest reorganizations of Earth's terrestrial
10 biome. Once thought to be globally synchronous in the late Miocene, site-specific studies have revealed differences in the
timing of the expansion and suggest that local conditions play a substantial role. Here, we examine the expansion of C₄
vegetation on the Indian Peninsula since the late Miocene by constructing a ~6 million year paleorecord with marine
sediment from the Bay of Bengal at Site U1445 drilled during International Ocean Discovery Program Expedition 353.
Analyses of element concentrations indicate the marine sediment originates from the Mahanadi River in the Core Monsoon
15 Zone (CMZ) of the Indian Peninsula. Hydrogen isotopes of the fatty acids of leaf waxes reveal an overall decrease in the
CMZ precipitation since the late Miocene. Carbon isotopes of the leaf wax fatty acids suggest C₄ vegetation on the Indian
Peninsula existed before the end of the Miocene, but expanded to even higher abundances during the mid-Pliocene to mid-
Pleistocene (3.5 to 1.5 Ma). Similar to the CMZ on the Indian Peninsula, a Pliocene expansion or re-expansion has
previously been observed in northwest Australia and in East Africa, suggesting that these tropical ecosystems surrounding
20 the Indian Ocean remained highly sensitive to changes in climate after the initial spread of C₄ plants in late Miocene.

1. Introduction

The expansion of plants using the C₄ photosynthetic pathway is one of the most dramatic reorganizations of the
global biome during the Neogene. A widespread late-Miocene expansion (8 to 6 Ma) is well documented and many studies
have interpreted the broadly synchronous timing as ecosystems adapting to decreasing pCO₂ (e.g., Ehleringer et al., 1991;
25 Ehleringer and Cerling, 1995; Cerling et al., 1993, 1997; Herbert et al., 2016). However, an increasing number of studies
have shown that the timing, regional patterns, rate and drivers of C₄ grassland expansion were much more diverse and
complex. Along with low pCO₂, a C₄ photosynthetic pathway is better adapted to higher temperature, aridity, seasonality,
and during disturbances such as flood, droughts, and fires (e.g., Edwards et al., 2010, and references therein). The interplay



of these parameters varies amongst regions. Resolving the precise timing and factors leading to major changes in vegetation
30 demands site-specific studies (Strömberg et al., 2011; Zhou et al., 2014).

Our study provides a novel piece of the puzzle in unraveling the complexities of C_4 expansion by constructing a 6
million year (Myr) record of C_4 vegetation and aridity on the Indian Peninsula. The marine sediment record is from
International Ocean Discovery Program (IODP) Site U1445 (17°44.72'N, 84°47.25'E; 2,503m water depth; Fig. 1A) drilled
in the Bay of Bengal (BoB) close to the mouths of the Mahanadi River. Lithologies at Site U1445 include calcareous fossils,
35 biosilica, silt, and clays (including glauconite), and are overall described as hemipelagic sediment (Clemens et al., 2016).
The Indian Monsoon dictates climate patterns in the Mahanadi River drainage basin: rainy summers, dry winters, and an
annual reversal of wind direction (Gadgil, 2003; Sarkar et al., 2015). Highly sensitive to the seasonal changes, more than
80% of runoff from the Mahanadi River into the BoB occurs during the summer (Chakrapani and Subramanian, 1990).

Previous reconstructions of Neogene C_4 expansion in regions affected by the Indian Monsoon use deposits
40 originating in the Himalayas and their piedmont regions (France-Lanord and Derry, 1994; Quade and Cerling, 1995; Quade
et al., 1995; Cerling et al., 1997; Freeman and Colarusso, 2001; Sanyal et al., 2004; Behrensmeyer et al., 2007; Galy et al.,
2010; Ghosh et al., 2017). The Mahanadi River drains a relatively low-elevation region of the Indian Peninsula distinct from
the nearby mountain ranges (e.g., the Western Ghats, the Himalaya, Indo-Burman ranges Fig. 1, Xie et al., 2006). With
minimal orographic precipitation in the Mahanadi River basin, rainfall in this “Core Monsoon Zone” (CMZ) represents the
45 mean behavior of the Indian Monsoon (Fig. 1; Ponton et al., 2012; Sarkar et al., 2015; Giosan et al., 2017, and references
therein).

Although agriculture dominates present-day vegetation, models predict natural flora of the Mahanadi basin would
be closed-canopy, moist deciduous forests and moist-to-dry woodlands with rare open spaces (Fig. 1C, Zorzi et al., 2015 and
references therein). Today the region encompasses a range of C_3 and C_4 vegetation, but proxies and models suggest that the
50 plant communities are highly sensitive to glacial-interglacial changes with nearly all flora utilizing a C_4 pathway during the
last glacial maximum (Galy et al., 2008; Phillips et al., 2014; Zorzi et al., 2015, and references therein). The behavior of
vegetation in the CMZ over million-year timescales is unknown.

Here, we use inorganic bulk geochemical analyses to fingerprint the origin of sediment at Site U1445 to be from the
Mahanadi River. Then we use bulk organic and compound-specific biomarkers at the same site, including carbon and
55 hydrogen isotope measurements of leaf wax fatty acids, to reconstruct the changes in C_4 vegetation and rainfall in the CMZ
of the Indian Peninsula over the last ~6 Myr (Fig. 2).

2. Methods

We constructed an age model for Site U1445 using CLAM software in R (Blaauw, 2010) to fit a locally weighted
spline to biostratigraphic and magnetostratigraphic ages (Clemens et al., 2016; Fig. S1). Our samples were collected from
60 the same hole in which the age model was constructed. We measured major, trace, and rare earth element concentrations on



30 bulk sediment samples spanning 0-6 Ma to determine sediment provenance (Dunlea et al., 2015; Appendix A). Then we analyzed bulk organics (Appendix B) as well as compound-specific biomarkers (Appendix C) from 57 samples to reconstruct hydrological and vegetation changes. Samples for biomarker analysis were collected from Site U1445 in pairs, visually targeting relatively light and dark layers at similar depths to capture the variability range on shorter timescales while
65 characterizing longer trends.

3. Results

The age model constructed at Hole U1445A suggests that long-term sedimentation rates have been overall continuous and fairly constant (Fig. S1). Shipboard scientists observed thin turbiditic sequences (~2-20cm thick) throughout Site U1445 and the expansion and dissociation of gas hydrates upon recovery that may muddle a higher-resolution record
70 (Clemens et al., 2016). However, Site U1445 has fewer and smaller turbidite deposits relative to other sites drilled in this region and the records spanning million-year timescales are likely relatively undisturbed.

To determine the provenance of the aluminosilicate fraction, we examined the proportions of Al, Ti, Sc, Nb, La, and Th concentrations, because other elements (e.g., Fe, K, Mg, Si, Zr, Hf) may be affected by continental weathering, sorting during transport, and post-depositional authigenic processes. The results from 30 samples have almost constant
75 element proportions of the selected elements, indicating that the aluminosilicate fraction of sediment not significantly varied over the past 6 Myr. The composition of the 30 samples, even amongst the light and dark layers, matches the composition of lithologies that comprise the Mahanadi basin such as Precambrian granite and gneisses of the Indian craton and associated sedimentary deposits (Sharma, 2009; Fig. S2; Table S1). Marine sediment deposits in other parts of the Bay of Bengal closer to the Krishna and Godavari Rivers or Ganges-Brahmaputra Rivers have a more mafic or highly variable composition that is
80 not observed at Site U1445 (Tripathy et al., 2014; Fig. S2). As such, we interpret our results as recording terrestrial changes in the CMZ, specifically the Mahanadi drainage basin.

The pairs of samples used for organic analyses are spaced ~28 m apart (~260 kyr intervals) and the adjacent light and dark layers within each pair were 0.2 m to 4.3 m apart in the sediment core (2 kyr to 46 kyr; Fig. S1). The color difference can be related to the total organic carbon content (wt%; TOC) content with darker layers having 1.0 to 2.8 times
85 more than adjacent lighter layers (Fig. 2A; Fig. S3; Table S2).

Long-chain normal fatty acids of leaf waxes are derived from land plants and are well preserved during transport and burial in marine sediment (Eglinton and Eglinton, 2008). We focus on the C₃₀ chain length to avoid possible contaminations from non-terrestrial sources that contribute shorter chain length fatty acids (Fig. S4; Table S3). The results of the $\delta^{13}\text{C}$ of C₃₀ fatty acid of leaf waxes ($\delta^{13}\text{C}_{\text{FA}}$) show a 5‰ increase from mid-Pliocene to mid-Pleistocene (3.5 to 1.5 Ma),
90 after which $\delta^{13}\text{C}_{\text{FA}}$ decreases and becomes more variable from 1.5 Ma to the present (Fig. 2B). The hydrogen isotope compositions of the leaf wax fatty acids ($\delta\text{D}_{\text{FA}}$) increase over the past 6 Myr, but have a wide range amongst light and dark



layers and shorter time intervals (Fig. 2C; Table S3). Before the mid-Pliocene (3.5 Myr) δD_{FA} ranges from -177‰ to -146‰ and after the mid-Pleistocene (1.5 Myr) the δD_{FA} increases to between -163‰ to -125‰ (Fig. 2C).

4. Discussion

95 4.1 C₄ Expansion on the Indian Peninsula

The $\delta^{13}C_{FA}$ of terrestrial plants is primarily a function of the photosynthetic pathway and isotopic composition of atmospheric CO₂ (e.g., Farquhar et al., 1989). In this study, the 5‰ increase in $\delta^{13}C_{FA}$ is greater than the reconstructed $\delta^{13}C$ of atmospheric CO₂ ($\leq 1\%$; Tipple et al., 2010), suggesting that a correction for $\delta^{13}C_{CO_2}$ would only slightly adjust our results. Thus we interpret $\delta^{13}C_{FA}$ as reflecting the amount of C₄ relative to C₃ vegetation produced in the CMZ.

100 Approximating typical $\delta^{13}C_{FA}$ of C₃ and C₄ plants (Chikaraishi et al., 2004; Ponton et al., 2012), we estimate that 36% to 68% (avg. 56% \pm 9% s.d.) of the vegetation in the CMZ utilized a C₄ photosynthetic pathway from 6 Ma until 3.5 Ma (Fig. S5). Thus, the environmental threshold for C₄ photosynthetic pathway had already been crossed before the end of the late Miocene. Later in the mid-Pliocene, the reconstruction shows another distinct expansion reaching 62% to 88% (avg. 80% \pm 8% s.d.) of C₄ vegetation in the early Pleistocene (Fig. 2B). The substantial change in vegetation from 3.5 to 1.5 Ma
105 suggests multiple steps of C₄ expansion in the CMZ, rather than a singular late-Miocene expansion. From 1.5 Ma to the present, the average proportion of C₄ vegetation decreased and became more variable (54% to 87%, avg. 71% \pm 11% s.d.; Fig. 2B), which may reflect the sensitivity of the region to glacial-interglacial variations observed in shorter records from this region (e.g., Zorzi et al., 2015, and references therein).

4.2 Aridification of the Indian Peninsula

110 The amount of precipitation, mixing of different air masses, and plant physiology can each vary the hydrogen isotopic composition of leaf wax fatty acids (δD_{FA} ; e.g., Eglinton and Eglinton, 2008). The mixing of two air masses with unique δD values was recently observed to drive δD of rainfall in New Delhi, India, but, similar to the amount of precipitation, the relatively depleted δD corresponded with wetter conditions (Hein et al., 2017). Thus, we corrected for the physiological effects of C₃ versus C₄ plants on δD_{FA} (Fig. S5; Fig. 2C), and interpreted the corrected δD_{FA} as a qualitative
115 proxy for aridity or the relative amount of precipitation. The δD_{FA} results suggest an overall drying of the CMZ on the Indian Peninsula over the past 6 Myr. The shorter-term scatter in the δD_{FA} record may reflect higher frequency variations in aridity or rainfall.



4.3 Global Patterns of C₄ Expansion

120 Untangling the triggers of C₄ expansions during the Neogene requires compiling records from many sites to identify
global versus local trends. Here, we compare our record with other compound-specific biomarker records of C₄ expansion at
sites in the Indian Ocean or adjacent land and seas.

125 Multiple proxy records document a late-Miocene C₄ expansion in the Ganges or Brahmaputra River basins such as
the Siwalik Group in northern Pakistan or BoB sites receiving outflow sediment (Fig. 3A France-Lanord and Derry, 1994;
Quade and Cerling, 1995; Cerling et al., 1997; Freeman and Colarusso, 2001; Sanyal et al., 2004; Behrensmeyer et al., 2007;
130 Ghosh et al., 2017). Collectively, the reported timing of C₄ expansions in the Himalaya region ranges from 9 to 5 Ma, most
commonly 8 to 6 Ma (Behrensmeyer et al., 2007). Rather than a uniform timing, detailed sampling of various deposits
around the Siwalik regions shows that C₄ vegetation expansion was staggered amongst nearby sub-environments with
different local conditions (Ghosh et al., 2017, and references therein). Another biomarker record documents a late-Miocene
expansion in a wide continental region north and west of the Arabian Sea (Site 722; Fig. 1A, Fig. 3B; Huang et al., 2007).
135 Once C₄ vegetation expanded at each of these sites, the records suggest there is overall little change in the amount of C₄
vegetation after the late Miocene.

In contrast, the CMZ of the Indian Peninsula and a few other records around the Indian Ocean document an
expansion of C₄ vegetation during the Pliocene (Fig. 3). Marine deposits in the Gulf of Aden originate from northeast Africa
and record a late-Miocene C₄ expansion, followed by a relapse to predominantly C₃ vegetation ~4.3 Ma and a re-expansion
135 of C₄ plants in the Pliocene (Site 231; Fig. 1A, Fig. 3C; Feakins et al., 2005, 2013; Liddy et al., 2016). The Pliocene re-
expansion is consistent with other records from tropical East Africa (e.g., Levin et al., 2004; Cerling et al., 2011). A C₄
expansion in the Pliocene is also observed in northwest Australia (Site 763A; Fig. 3E; Andrae et al., 2018). There is little
evidence of significant C₄ vegetation prior to the Pliocene, suggesting a relatively late onset of C₄ vegetation expansion in
northwest Australia (Fig. 3).

140 Collectively, a significant regional expansion in the Pliocene, distinctly after the first late-Miocene expansion, is
common at least amongst tropical East Africa, Northwest Australia, and the Indian Peninsula. Farther from the Indian
Ocean, there is also evidence that East and Central Asia also experienced multiple steps of C₄ expansion through the
Pliocene, depending on local sub-climates (e.g., An et al., 2005; Passey et al., 2009; Zhou et al., 2014). The modes of climate
variability around the Indian Ocean likely differed throughout the Pliocene and may have set the stage for a regional, multi-
145 step reorganization of the terrestrial biome.

4.4 Triggers of C₄ Expansion in the Pliocene

Many studies hypothesize that the widespread expansion of C₄ vegetation in the late Miocene was triggered by
pCO₂ decreasing below a temperature-dependent threshold (Herbert et al., 2016 and references therein). Since C₄-dominated
ecosystems are favored under low pCO₂ and higher temperatures, the expansion was proposed to occur earlier at lower



150 latitudes and later cross the pCO₂ threshold at cooler, higher latitudes (e.g., Cerling et al., 1997). During the Pliocene, pCO₂
also decreased (Fedorov et al., 2013), but ecosystems at higher latitudes or elevations remained relatively stable, perhaps
sufficiently past the pCO₂ threshold. In contrast, the tropical ecosystems adjacent to the Indian Ocean seem to be more
sensitive, suggesting pCO₂ is likely not the primary driver of the Pliocene C₄ expansion.

Other possible triggers for C₄ expansion (aridity, seasonality, flood, droughts, and fires) depend on precipitation
155 patterns. In the modern era, a complex interplay of multiple modes of variability dictate the unique seasonal and multi-
decadal precipitation patterns in the regions surrounding the Indian Ocean. For example, rainfall on the Indian Peninsula
follows quintessential monsoon behavior, but is also tied to the Inter-Tropical Convergence Zone (ITCZ), Walker
Circulation, and the Indian Ocean Dipole (IOD; Wang et al., 2017). The biannual rains of the (semi)arid tropical East Africa
are related to the ITCZ, monsoon winds, sea surface temperature (SST), and Walker Circulation (e.g., Williams and Funk,
160 2011; Tierney et al., 2015; Yang et al., 2015). Monsoon rains annually quench northern Australia, but the El Niño Southern
Oscillation (ENSO), Walker Circulation, and the amount of Indonesian Throughflow (ITF) better explain the precipitation in
other parts of Australia (Ummenhofer et al., 2009, 2011a, 2011b).

Since a single process cannot explain the precipitation patterns surrounding the Indian Ocean, the interplay of many
processes likely changed during the Pliocene. Along with decreasing pCO₂, the ITF constricted (Cane and Molnar, 2001;
165 Karas et al., 2009; Christensen et al., 2017) and SST gradients changed (Wara et al., 2005; Zhang et al., 2014; Burls and
Fedorov, 2017), which would have modulated the monsoon dynamics and their interaction with the ITCZ, ENSO, IOD, and
other modes of variability. Manifesting as increased aridity, seasonality, droughts, flooding, or fires, the changes in the
hydroclimate variability over the Pliocene led to conditions more conducive to C₄ vegetation in certain tropical regions
adjacent to the Indian Ocean.

170 **5. Conclusion**

Our study provides a piece of the puzzle in unraveling the complexities of C₄ expansion and adds nuance to the
discussion of triggering mechanism. Although C₄ vegetation was established in the CMZ on the Indian Peninsula before the
end of the Miocene, the results of this study show another significant expansion in the Pliocene (~3.5 to 1.5 Ma). The latter
expansion is not observed in many records from the orographically-wet Himalaya emphasizing the spatial heterogeneities in
175 C₄ vegetation response – even within the same monsoon system. However, other regions adjacent to the Indian Ocean, such
as tropical East Africa and Northwest Australia, corroborate the observed expansion in the CMZ of the Indian Peninsula and
show C₄ vegetation patterns sensitive to the changes in hydroclimate during the Pliocene.



6. Appendices

Appendix A: Analytical Procedures - Inorganic Analyses of bulk major, trace, rare earth element concentrations

180 The samples we analyzed for major, trace, and rare earth element concentrations were originally collected for
moisture and density (MAD) measurements onboard the JOIDES Resolution during IODP Expedition 353. Each sample was
collected with a 2 cm diameter plastic syringe that fits into the top of a 10 cm³ volume glass vial, allowing for the vial to be
completely filled with sediment (Clemens et al., 2016). The samples were dried in a convective oven at 105°C ± 5°C for 24
hours (Clemens et al., 2016). The remaining sample preparation, digestions, and analyses were conducted at Boston
185 University and a detailed description of the analytical geochemical procedures are presented in Dunlea et al. (2015). In
summary here, sediment samples were hand-powdered with an agate mortar and pestle. For major and certain trace elements,
sample powders were digested by flux fusion (Murray et al., 2000) and analyzed by inductively coupled plasma-emission
spectrometry (ICP-ES). For analysis of additional trace and rare earth elements, sample powders were dissolved in a heated
acid cocktail (HNO₃, HCl, and HF, with later additions of HNO₃ and H₂O₂ after samples were dried down) under clean-lab
190 conditions and analyzed by inductively couple plasma-mass spectrometry (ICP-MS). Three separate digestions of a matrix-
matched in-house sediment standard were analyzed with each batch and determined precision [(standard
deviation)/(average) x 100] was ~2% of the measured value for each element. The international Standard Reference Material
BHVO-2 was analyzed as an unknown with each batch and results were consistently found to be accurate within precision
for each element.

195 Appendix B: Analytical Procedures - Carbon and nitrogen content and isotopes

Analyses of the abundance of total carbon (TC), total inorganic carbon (TIC), total organic carbon (TOC), nitrogen
(N), the δ¹³C of the TOC, and the δ¹⁵N of the N component were performed at Woods Hole Oceanographic Institution and
methods are described in Whiteside et al. (2011). In brief here, samples for TOC were weighed into tared silver boats and
then acidified to remove carbonates in a closed desiccator for 3 days at 60-65°C over concentrated hydrochloric acid. All
200 samples were flash combusted in a Costech 4010 Elemental Analyzer coupled via a Finnigan-MAT Conflo-II interface to a
Thermo DeltaVPlus isotope ratio mass spectrometer. Data were recorded and integrated using the Isodat software package.
Post-run calculations were performed for blank corrections, quantifications, and final calibrations.

Appendix C: Analytical Procedures - Compound specific biomarkers abundances and isotopes

The analyses of compound-specific biomarkers were performed at Brown University (e.g., Daniels et al., 2017).
205 Samples were freeze-dried and lipids were extracted from 3.5 to 4.5 g of sediment using a Dionex 350 Accelerated Solvent
Extractor (ASE) with dichloromethane:methanol (9:1 v/v). The fatty acids in the total lipid extract were separated from the
neutral lipids using aminopropyl silica gel chromatography, eluting with a dichloromethane:isopropanol solution followed
by ether with 5% acetic acid.



210 The fatty acids were methylated to form fatty acid methyl ester (FAME) by dissolving dried down acid fraction in
in ~0.3 mL of toluene and ~1mL of 5:95 acetyl chloride:methanol. Nitrogen replaced the headspace in the vial before they
were capped tightly and heated at 60°C for 12 hours. Once the reaction was complete, the FAMEs were separated from the
water by-products formed during the methylation reaction. Sample received ~1mL of synthetic saline solution (50g NaCl/L
of double-distilled water) and ~1mL of hexane, were vigorously shaken, and then allowed to rest until the hexane separated
from the water. The hexane fraction was pipetted into a new vial, avoiding the water. Another ~1mL of hexane was added to
215 the sample, shaken, and pipetted into the new vial. To clean the solution and isolate the fatty acids, samples were run
through a second silica gel column, eluting with hexane to remove unwanted acids and then DCM to acquire the clean
FAME fraction.

The neutral lipid fraction of the total lipid extract was further separated into the n-alkane fraction (N1),
ketone/sterol fraction (N2, alkenones), and the alcohol fraction (N3, GDGTs and diols) eluting with hexane, DCM, and
220 methanol, respectively. The FAME, alkanes (N1), and alkenone (N2) fractions were analyzed on an Agilent 6890 gas
chromatograph with a flame ionization detector (GC-FID). To quantify alkane (N1) abundances, a hexamethylbenzene
internal standard was analyzed with each sample. To quantify alkenone (N2) abundances, an 18-pentatriacontane standard
was used. Sample blanks were analyzed with every batch.

The isotope ratios of the FAME fraction ($\delta D_{n\text{-acid}}$ and $\delta^{13}C_{n\text{-acid}}$) were measured on a Thermo Finnigan Delta + XL
225 isotope ratio mass spectrometer with a HP 6890 gas chromatograph and a high-temperature pyrolysis reactor for sample
introduction. For δD , three injections of each sample were analyzed and two injections of each sample were analyzed for
 $\delta^{13}C$. Between every six injections, a standard mixture containing C_{16} , C_{18} , C_{22} , C_{26} , and C_{28} n-acids was analyzed to monitor
instrument accuracy and precision. Analytical uncertainty was calculated by [standard deviation/average] of the injections
and is typically less than 3% for δD and less than 1% for $\delta^{13}C$. The standard deviations are reported in Table S3. For every
230 instrument run, samples were analyzed in random order.

Data Availability

Data is included in the supplementary tables and will be made publically available in the NSF funded EarthChem
database (<https://www.earthchem.org/>) maintained by the Interdisciplinary Earth Data Alliance (IEDA) at the Lamont-
Doherty Earth Observatory of Columbia University.

235 Author Contribution

A.G.D. participated in the IODP Expedition 353 sampling party, performed the geochemical analyses, and lead
writing and revisions of the manuscript. L.G. participated on IODP Expedition 353, was involved in the project's
conceptualization, sample acquisition, and provided supervision. Y.H. also participated on IODP Expedition 353, was



involved in the project's conceptualization, provided resources and funding acquisition, advised on the methodology,
240 supervision, and aided in interpretation of data.

Competing Interests

The authors declare that they have no conflict of interest.

Acknowledgements

We thank Raj Kumar Singh (IIT Bhubaneswar, India) for providing Mahanadi sediment samples, X. Wang, R.
245 Tarozo, and M. Da Rosa Alexandre at Brown Univ. and T. Ireland at Boston Univ. for their analytical assistance and as well
as S. Clemens, K. Thirumalai, V. Galy, and C. Ummenhofer for discussions and advice. This research used samples and
data provided by the International Ocean Discovery Program. Funding for this research was provided by the Ocean and
Climate Change Institute Postdoctoral Scholarship at Woods Hole Oceanographic Institution to AGD, and the U.S. National
Science Foundation to LG (NSF OCE-0652315). USSSP post-cruise support was provided to Exp. 353 shipboard
250 participants LG and YH.

References

- An, Z., Huang, Y., Liu, W., Guo, Z., Clemens, S., Li, L., Prell, W., Youfeng, N., Yanjun, C., Weijian, Z., Benhai, L., Qingle,
Z., Yunning, C., Xiaoke, Q., Hong, C. and Zhenkun, W.: Multiple expansions of C4 plant biomass in East Asia
since 7 Ma coupled with strengthened monsoon circulation, *Geology*, 33(9), 705, doi:10.1130/g21423.1, 2005.
- 255 Andrae, J. W., McInerney, F. A., Polissar, P. J., Sniderman, J. M. K., Howard, S., Hall, P. A. and Phelps, S. R.: Initial
Expansion of C4 Vegetation in Australia During the Late Pliocene, *Geophys. Res. Lett.*, 45(10), 4831–4840,
doi:10.1029/2018GL077833, 2018.
- Behrensmeyer, A. K., Quade, J., Cerling, T. E., Kappelman, J., Khan, I. A., Copeland, P., Roe, L., Hicks, J., Stubblefield, P.,
Willis, B. J. and Latorre, C.: The structure and rate of late Miocene expansion of C4 plants: Evidence from lateral
260 variation in stable isotopes in paleosols of the Siwalik Group, northern Pakistan, *Geol. Soc. Am. Bull.*, 119(11-12),
1486–1505, doi:10.1130/B26064.1, 2007.
- Blaauw, M.: Methods and code for 'classical' age-modeling of radiocarbon sequences, *Quat. Geochron.*, 5, 512-518, doi:
10.1016/j.quageo.2010.01.002, 2010.
- Burls, N. J. and Fedorov, A. V.: Wetter subtropics in a warmer world: Contrasting past and future hydrological cycles,
265 *PNAS*, 114(49), 12888–12893, doi:10.1073/pnas.1703421114, 2017.



- Cane, M. A. and Molnar, P.: Closing of the Indonesian seaway as a precursor to east African aridification around 3–4 million years ago, *Nature*, 411(6834), 157–162, doi:10.1038/35075500, 2001.
- Cerling, T. E., Wang, Y. and Quade, J.: Expansion of C4 ecosystems as an indicator of global ecological change in the late Miocene, *Nature*, 361(6410), 344–345, doi:10.1038/361344a0, 1993.
- 270 Cerling, T. E., Harris, J. M., MacFadden, B. J., Leakey, M. G., Quade, J., Eisenmann, V. and Ehleringer, J. R.: Global vegetation change through the Miocene/Pliocene boundary, *Nature*, 389(6647), 153–158, doi:10.1038/38229, 1997.
- Cerling, T. E., Wynn, J. G., Andanje, S. A., Bird, M. I., Korir, D. K., Levin, N. E., Mace, W., Macharia, A. N., Quade, J. and Remien, C. H.: Woody cover and hominin environments in the past 6 million years, *Nature Geosci.*, 476(7358), 51–56, doi:10.1038/nature10306, 2011.
- 275 Chakrapani, G. J. and Subramanian, V.: Factors controlling sediment discharge in the Mahanadi River Basin, India, *Journal of Hydrology*, 117(1-4), 169–185, doi:10.1016/0022-1694(90)90091-b, 1990.
- Chikaraishi, Y., Naraoka, H. and Poulson, S. R.: Hydrogen and carbon isotopic fractionations of lipid biosynthesis among terrestrial (C3, C4 and CAM) and aquatic plants, *Phytochemistry*, 65(10), 1369–1381, doi:10.1016/j.phytochem.2004.03.036, 2004.
- 280 Christensen, B. A., Renema, W., Henderiks, J., De Vleeschouwer, D., Groeneveld, J., Castañeda, I. S., Reuning, L., Bogus, K., Auer, G., Ishiwa, T., McHugh, C. M., Gallagher, S. J., Fulthorpe, C. S. IODP Expedition 356 Scientists: Indonesian Throughflow drove Australian climate from humid Pliocene to arid Pleistocene, *Geophys. Res. Lett.*, 44(13), 6914–6925, doi:10.1002/2017GL072977, 2017.
- Clemens, S. C., Kuhnt, W., LeVay, L. J., Anand, P., Ando, T., Bartol, M., Bolton, C. T., Ding, X., Gariboldi, K., Giosan, L., 285 Hathorne, E. C., Huang, Y., Jaiswal, P., Kim, S., Kirkpatrick, J. B., Littler, K., Marino, G., Martinez, P., Naik, D., Peketi, A., Phillips, S. C., Robinson, M. M., Romero, O. E., Sagar, N., Taladay, K. B., Taylor, S. N., Thirumalai, K., Uramoto, G., Usui, Y., Wang, J., Yamamoto, M. and Zhou, L.: Indian Monsoon Rainfall, *Proc. of IODP*, 353, doi:10.14379/iodp.proc.353.101.2016, 2016.
- Daniels, W. C., Russell, J. M., Giblin, A. E., Welker, J. M., Klein, E. S. and Huang, Y.: Hydrogen isotope fractionation in 290 leaf waxes in the Alaskan Arctic tundra, *Geochim. Cosmochim. Acta*, 213, 216–236, doi:10.1016/j.gca.2017.06.028, 2017.
- Dunlea, A. G., Murray, R. W., Sauvage, J., Spivack, A. J., Harris, R. N. and D'Hondt, S.: Dust, volcanic ash, and the evolution of the South Pacific Gyre through the Cenozoic, *Paleocean.*, 30, 1078–1099, doi:10.1002/2015PA002829, 2015.
- 295 Edwards, E. J., Osborne, C. P., Strömberg, C., Smith, S. A. and Consortium, C. G.: The origins of C4 grasslands: integrating evolutionary and ecosystem science, *Science*, 328(5978), 587–591, doi:10.1126/science.1177216, 2010.
- Ehleringer, J. R. and Cerling, T. E.: Atmospheric CO2 and the ratio of intercellular to ambient CO2 concentrations in plants, *Tree Physiology*, 15, 105–111, 1995.



- Ehleringer, J. R., Sage, R. F., Flanagan, L. B. and Pearcy, R. W.: Climate change and the evolution of C4 photosynthesis, Mar. Geol., 6(3), 95–99, doi:10.1016/0169-5347(91)90183-X, 1991.
- 300 Eglinton, T. I. and Eglinton, G.: Molecular proxies for paleoclimatology, Earth Planet. Sci. Let., 275(1-2), 1–16, doi:10.1016/j.epsl.2008.07.012, 2008.
- Farquhar, G. D., Ehleringer, J. R. and Hubick, K. T.: Carbon isotope discrimination and photosynthesis, Annu. Rev. Plant Physiol. Plant Mol. Biol., 40(1), 503–537, doi:10.1146/annurev.pp.40.060189.002443, 1989.
- 305 Feakins, S. J., DeMenocal, P. B. and Eglinton, T. I.: Biomarker records of late Neogene changes in northeast African vegetation, Geology, 33(12), 977–4, doi:10.1130/G21814.1, 2005.
- Feakins, S. J., Levin, N. E., Liddy, H. M., Sieracki, A., Eglinton, T. I. and Bonnefille, R.: Northeast African vegetation change over 12 m.y, Geology, 41(3), 295–298, doi:10.1130/G33845.1, 2013.
- Fedorov, A. V., Brierley, C. M., Lawrence, K. T., Liu, Z., Dekens, P. S. and Ravelo, A. C.: Patterns and mechanisms of early Pliocene warmth, Nature Geosci., 496(7443), 43–49, doi:10.1038/nature12003, 2013.
- 310 France-Lanord, C. and Derry, L. A.: $\delta^{13}\text{C}$ of organic carbon in the Bengal Fan: Source evolution and transport of C3 and C4 plant carbon to marine sediments, Geochim. Cosmochim. Acta, 58(21), 4809–4814, doi:10.1016/0016-7037(94)90210-0, 1994.
- Freeman, K. H. and Colarusso, L. A.: Molecular and isotopic records of C4 grassland expansion in the late miocene, Geochim. Cosmochim. Acta, 65(9), 1439–1454, doi:10.1016/s0016-7037(00)00573-1, 2001.
- 315 Gadgil, S.: The Indian Monsoon and its Variability, Annu. Rev. Earth Planet. Sci., 31(1), 429–467, doi:10.1146/annurev.earth.31.100901.141251, 2003.
- Galy, V., France-Lanord, C., Peucker-Ehrenbrink, B. and Huyghe, P.: Sr–Nd–Os evidence for a stable erosion regime in the Himalaya during the past 12Myr, Earth Planet. Sci. Let., 290(3-4), 474–480, doi:10.1016/j.epsl.2010.01.004, 2010.
- 320 Galy, V., François, L., France-Lanord, C., Faure, P., Kudrass, H., Palhol, F. and Singh, S. K.: C4 plants decline in the Himalayan basin since the Last Glacial Maximum, Quat. Sci. Rev., 27(13-14), 1396–1409, doi:10.1016/j.quascirev.2008.04.005, 2008.
- Ghosh, S., Sanyal, P. and Kumar, R.: Evolution of C4 plants and controlling factors: Insight from n-alkane isotopic values of NW Indian Siwalik paleosols, Org. Geochem., 110, 110–121, doi:10.1016/j.orggeochem.2017.04.009, 2017.
- 325 Giosan, L., Ponton, C., Usman, M., Blusztajn, J., Fuller, D. Q., Galy, V., Haghypour, N., Johnson, J. E., McIntyre, C., Wacker, L. and Eglinton, T. I.: Massive erosion in monsoonal central India linked to late Holocene land cover degradation, Earth Surf. Dynam., 5(4), 781–789, doi:10.5194/esurf-5-781-2017, 2017.
- Hein, C. J., Galy, V., Galy, A., France-Lanord, C., Kudrass, H. and Schwenk, T.: Post-glacial climate forcing of surface processes in the Ganges–Brahmaputra river basin and implications for carbon sequestration, Earth Planet. Sci. Let., 478, 89–101, doi:10.1016/j.epsl.2017.08.013, 2017.
- 330 Herbert, T. D., Lawrence, K. T., Tzanova, A., Peterson, L. C., Caballero-Gill, R. and Kelly, C. S.: Late Miocene global cooling and the rise of modern ecosystems, Nat. Geosci., 9(11), 843–847, doi:10.1038/ngeo2813, 2016.



- Huang, Y., Clemens, S. C., Liu, W., Wang, Y. and Prell, W. L.: Large-scale hydrological change drove the late Miocene C4
plant expansion in the Himalayan foreland and Arabian Peninsula, *Geology*, 35(6), 531–534,
335 doi:10.1130/G23666A.1, 2007.
- Karas, C., Nürnberg, D., Gupta, A. K., Tiedemann, R., Mohan, K. and Bickert, T.: Mid-Pliocene climate change amplified
by a switch in Indonesian subsurface throughflow, *Nat. Geosci.*, 2(6), 434–438, doi:10.1038/ngeo520, 2009.
- Levin, N. E., Quade, J., Simpson, S. W., Semaw, S. and Rogers, M.: Isotopic evidence for Plio–Pleistocene environmental
change at Gona, Ethiopia, *Earth Planet. Sci. Lett.*, 219(1–2), 93–110, doi:10.1016/S0012-821X(03)00707-6, 2004.
- 340 Liddy, H. M., Feakins, S. J. and Tierney, J. E.: Cooling and drying in northeast Africa across the Pliocene, *Earth Planet. Sci.*
Let., 449, 430–438, doi:10.1016/j.epsl.2016.05.005, 2016.
- Murray, R., Miller, D. J. and Kryc, K.: Analysis of major and trace elements in rocks, sediments, and interstitial waters by
inductively coupled plasma–atomic emission spectrometry (ICP–AES), *ODP Tech. Note*, 29, 1–27, 2000.
- Passey, B. H., Ayliffe, L. K., Kaakinen, A., Zhang, Z., Eronen, J. T., Zhu, Y., Zhou, L., Cerling, T. E. and Fortelius, M.:
345 Strengthened East Asian summer monsoons during a period of high-latitude warmth? Isotopic evidence from Mio-
Pliocene fossil mammals and soil carbonates from northern China, *Earth Planet. Sci. Lett.*, 277(3–4), 443–452,
doi:10.1016/j.epsl.2008.11.008, 2009.
- Phillips, S. C., Johnson, J. E., Giosan, L. and Rose, K.: Monsoon-influenced variation in productivity and lithogenic
sediment flux since 110 ka in the offshore Mahanadi Basin, northern Bay of Bengal, *Marine and Petroleum*
350 *Geology*, 58(PA), 502–525, doi:10.1016/j.marpetgeo.2014.05.007, 2014.
- Ponton, C., Giosan, L., Eglinton, T. I., Fuller, D. Q., Johnson, J. E., Kumar, P. and Collett, T. S.: Holocene aridification of
India, *Geophys. Res. Lett.*, 39(3), L03704, doi:10.1029/2011GL050722, 2012.
- Quade, J. and Cerling, T. E.: Expansion of C4 grasses in the Late Miocene of Northern Pakistan: evidence from stable
isotopes in paleosols, *Palaeogeogr. Palaeoclimatol. Palaeoecol.*, 115, 91–116, doi:10.1016/0031-0182(94)00108-K,
355 1995.
- Quade, J., Cater, J. M. L., Ojha, T. P., Adam, J. and Harrison, T. M.: Late Miocene environmental change in Nepal and the
northern Indian subcontinent: Stable isotopic evidence from paleosols, *Geol. Soc. Am. Bull.*, 107(12), 1381–1397,
doi:10.1130/0016-7606(1995)107<1381:LMECIN>2.3.CO;2, 1995.
- Sanyal, P., Bhattacharya, S. K., Kumar, R., Ghosh, S. K. and Sangode, S. J.: Mio–Pliocene monsoonal record from
360 Himalayan foreland basin (Indian Siwalik) and its relation to vegetational change, *Palaeogeogr. Palaeoclimatol.*
Palaeoecol., 205(1–2), 23–41, doi:10.1016/j.palaeo.2003.11.013, 2004.
- Sarkar, S., Prasad, S., Wilkes, H., Riedel, N., Stebich, M., Basavaiah, N. and Sachse, D.: Monsoon source shifts during the
drying mid-Holocene: Biomarker isotope based evidence from the core 'monsoon zone' (CMZ) of India, *Quat. Sci.*
Rev., 123(C), 144–157, doi:10.1016/j.quascirev.2015.06.020, 2015.
- 365 Sharma, R. S.: Cratons of the Indian Shield, in *Cratons and Fold Belts of India*, vol. 127, pp. 41–115, Springer Berlin
Heidelberg, Berlin, Heidelberg, 2009.



- Strömberg, C. A. E.: Evolution of Grasses and Grassland Ecosystems, *Annu. Rev. Earth Planet. Sci.*, 39(1), 517–544, doi:10.1146/annurev-earth-040809-152402, 2011.
- 370 Tierney, J. E., Ummenhofer, C. C. and DeMenocal, P. B.: Past and future rainfall in the Horn of Africa, *Science Advances*, 1(9), e1500682–9, doi:10.1126/sciadv.1500682, 2015.
- Tipple, B. J., Meyers, S. R. and Pagani, M.: Carbon isotope ratio of Cenozoic CO₂: A comparative evaluation of available geochemical proxies, *Paleocean.*, 25(3), 129–11, doi:10.1029/2009PA001851, 2010.
- Tripathy, G. R., Singh, S. K. and Ramaswamy, V.: Major and trace element geochemistry of Bay of Bengal sediments: Implications to provenances and their controlling factors, *Palaeogeogr. Palaeoclimatol. Palaeoecol.*, 397(C), 20–30, doi:10.1016/j.palaeo.2013.04.012, 2014.
- 375 Ummenhofer, C. C., Gupta, Sen, A., Briggs, P. R., England, M. H., McIntosh, P. C., Meyers, G. A., Pook, M. J., Raupach, M. R. and Risbey, J. S.: Indian and Pacific Ocean Influences on Southeast Australian Drought and Soil Moisture, *J. Climate*, 24(5), 1313–1336, doi:10.1175/2010JCLI3475.1, 2011a.
- Ummenhofer, C. C., Gupta, Sen, A., Li, Y., Taschetto, A. S. and England, M. H.: Multi-decadal modulation of the El Niño–Indian monsoon relationship by Indian Ocean variability, *Environ. Res. Lett.*, 6(3), 034006–9, doi:10.1088/1748-9326/6/3/034006, 2011b.
- 380 Ummenhofer, C. C., Gupta, Sen, A., Taschetto, A. S. and England, M. H.: Modulation of Australian Precipitation by Meridional Gradients in East Indian Ocean Sea Surface Temperature, *J. Climate*, 22(21), 5597–5610, doi:10.1175/2009JCLI3021.1, 2009.
- 385 Wara, M. W., Ravelo, A. C. and Delaney, M. L.: Permanent El Niño-Like Conditions During the Pliocene Warm Period, *Science*, 309(5735), 758–761, doi:10.1126/science.1112596, 2005.
- Wang, P. X., Bin Wang, Cheng, H., Fasullo, J., Guo, Z., Kiefer, T. and Liu, Z.: The global monsoon across time scales: Mechanisms and outstanding issues, *Earth-Sci Rev*, 174, 84–121, doi:10.1016/j.earscirev.2017.07.006, 2017.
- Williams, A. P. and Funk, C.: A westward extension of the warm pool leads to a westward extension of the Walker circulation, drying eastern Africa, *Climate Dynamics*, 37(11-12), 2417–2435, doi:10.1007/s00382-010-0984-y, 2011.
- 390 Whiteside, J. H., Olsen, P. E., Eglinton, T. I., Cornet, B., McDonald, N. G. and Huber, P.: Pangean great lake paleoecology on the cusp of the end-Triassic extinction, *Palaeogeogr. Palaeoclimatol. Palaeoecol.*, 301(1-4), 1–17, doi:10.1016/j.palaeo.2010.11.025, 2011.
- 395 Xie, S.-P., Xu, H., Saji, N. H., Wang, Y. and Liu, W. T.: Role of Narrow Mountains in Large-Scale Organization of Asian Monsoon Convection, *J. Climate*, 19(14), 3420–3429, doi:10.1175/jcli3777.1, 2006.
- Yang, W., Seager, R., Cane, M. A. and Lyon, B.: The Annual Cycle of East African Precipitation, *J. Climate*, 28(6), 2385–2404, doi:10.1175/JCLI-D-14-00484.1, 2015.
- Zhang, Y. G., Pagani, M. and Liu, Z.: A 12-Million-Year Temperature History of the Tropical Pacific Ocean, *Science*, 400 344(6179), 84–87, doi:10.1126/science.1246172, 2014.

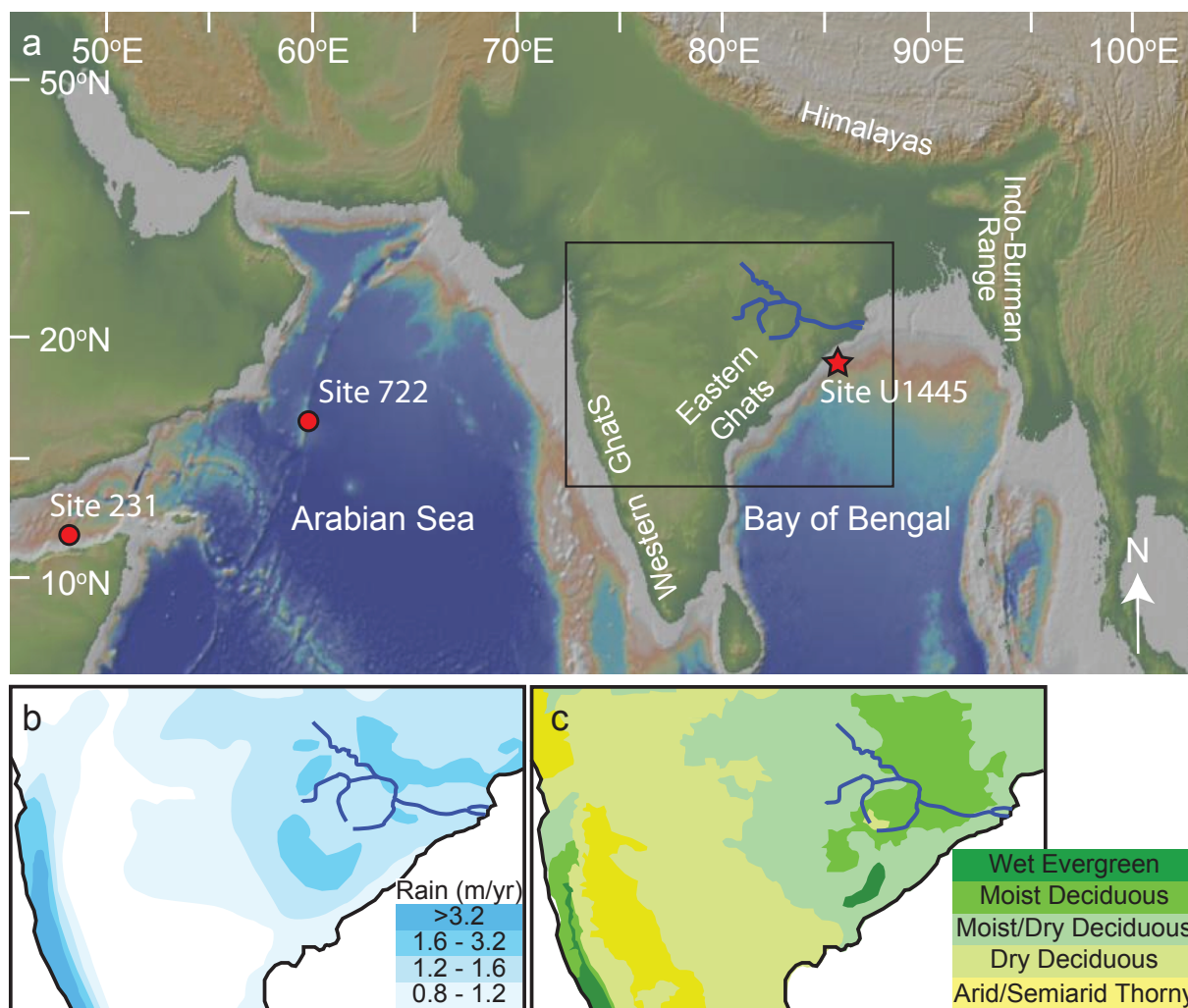


- Zhou, B., Shen, C., Sun, W., Bird, M., Ma, W., Taylor, D., Liu, W., Peterse, F., Yi, W. and Zheng, H.: Late Pliocene–Pleistocene expansion of C4 vegetation in semiarid East Asia linked to increased burning, *Geology*, 42(12), 1067–1070, doi:10.1130/g36110.1, 2014.
- 405 Zorzi, C., Goñi, M. F. S., Anupama, K., Prasad, S., Hanquiez, V., Johnson, J. and Giosan, L.: Indian monsoon variations during three contrasting climatic periods: The Holocene, Heinrich Stadial 2 and the last interglacial-glacial transition, *Quat. Sci. Rev.*, 125(C), 50–60, doi:10.1016/j.quascirev.2015.06.009, 2015.



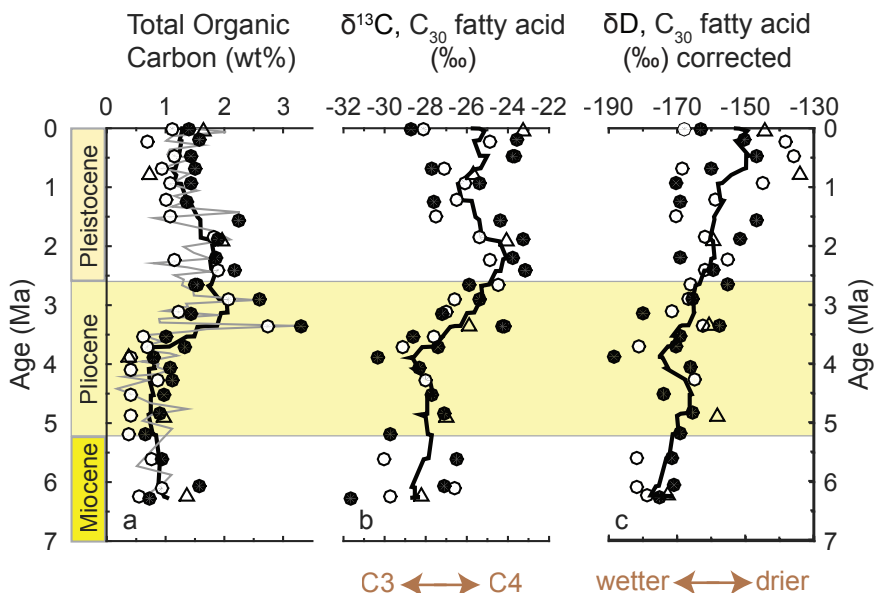
410

Figure 1. (a) Location of IODP Site U1445 in the Bay of Bengal (red star). Site 231 in the Gulf of Aden and Site 722 in the Arabian Sea are plotted for reference (red dots). Topography and bathymetry are represented in the background map. The Mahanadi River and main tributaries are traced in dark blue and the region outlined by the box is zoomed-in for Figures 1a and 1c, which are modified from Ponton et al. (2012). (b) average annual rainfall (m/year) and (c) natural ecosystems in the region including the Mahanadi River drainage basin.





415 Figure 2. Analyses of 57 samples from Site U1445 in the Bay of Bengal. Black and white dots are pairs of samples from relatively
 420 dark and light layers, respectively, at a similar depth. Triangles are samples not in pairs. Black curves are a 9-point moving
 average of all samples. Black text labels the data and brown text is our interpretations. (a) total organic carbon (wt. %). The grey
 line represents shipboard measurements (Clemens et al., 2016). (b) carbon isotope values of C₃₀ fatty acids from leaf waxes
 (δ¹³C_{FA}, per mil), (c) hydrogen isotope values of C₃₀ fatty acids from leaf waxes (δD_{FA}, per mil). The yellow horizontal band
 highlights the Pliocene epoch.





425 **Figure 3.** (a) $\delta^{13}\text{C}$ of C_{33} -alkanes from Siwalik paleosols in Northern Pakistan (white dots) and from sediment at Site 717 in the
430 Bengal Fan (black dots; Freeman and Colarusso, 2001). (b) $\delta^{13}\text{C}$ of C_{31} -alkanes at Site 722 in the Arabian Sea (Huang et al., 2007),
which integrates vegetation variability from north and east of the Arabian Sea. (c) $\delta^{13}\text{C}$ of C_{28} -fatty acids at Site 231 in the Gulf of
Aden, which records vegetation in East Africa (Feakins et al., 2013; Liddy et al., 2016). (d) $\delta^{13}\text{C}$ of C_{30} -fatty acid at Site U1445 in
the Bay of Bengal, which records vegetation from the Mahanadi basin on the Indian Peninsula (this study). (e) $\delta^{13}\text{C}$ of C_{33} -alkanes
from northwest Australia (Andrae et al., 2018). Brown arrows point out the late-Miocene C_4 expansion in Northern Pakistan,
Arabian Sea, and Gulf of Aden as well as the Pliocene C_4 expansion in northeast Africa and the Indian Peninsula.

